Spin-glass behaviour, thermal expansion anomaly and spin fluctuations in $Y_{20}(Mn_{1-x}Fe_x)_{80}$ amorphous alloys

1999 J. Phys.: Condens. Matter 11 4053

(http://iopscience.iop.org/0953-8984/11/20/312)

J. Phys.: Condens. Matter **11** (1999) 4053–4062. Printed in the UK PII: S0953-8984(99)01262-X

Spin-glass behaviour, thermal expansion anomaly and spin fluctuations in $Y_{20}(Mn_{1-x}Fe_x)_{80}$ amorphous alloys

M Ohta†, A Fujita†, K Fukamichi†, Y Obi‡ and H Fujimori‡

† Department of Materials Science, Graduate School of Engineering, Tohoku University, Aoba-yama 02, Sendai 980-8579, Japan

‡ Institute for Materials Research, Tohoku University, Sendai 980-8577, Japan

E-mail: mota@maglab.material.tohoku.ac.jp (M Ohta)

Received 26 January 1999

Abstract. The spin-glass behaviour and the thermal expansion anomaly in annealed $Y_{20}(Mn_{1-x}Fe_x)_{80}$ amorphous alloys have been investigated. The spin freezing temperature T_g shows a minimum at around $x = 0.50$, consistent with the theoretical investigation. The sign of the paramagnetic Curie temperature θ_p indicates that the average exchange interaction is antiferromagnetic in the Mn-rich concentration region and gradually becomes ferromagnetic with increasing x. The minimum of T_g occurs at the concentration where the sign of θ_p changes.

The spontaneous volume magnetostriction is negligibly small in the Mn-rich concentration region and becomes larger with increasing x. These results are explained by the change in the spin fluctuation characteristics. In the Fe-rich concentration region, the thermal expansion anomaly takes place even in the paramagnetic temperature range due to the single-site spin fluctuation.

1. Introduction

It has been reported that a spin-glass behaviour is established in Y–Fe [1–8] and Y–Mn [9, 10] amorphous alloys at low temperatures. Y–Fe amorphous alloys have a positive paramagnetic Curie temperature θ_p [4, 6], showing that the average exchange interaction between the nearest neighbours is ferromagnetic. Moreover, as-prepared samples show a transition from a paramagnetic state to a spin-glass state with decreasing temperature, whereas their annealed samples exhibit a re-entrant spin-glass behaviour [4–6]. The re-entrant spin-glass behaviour is also induced in the as-prepared samples by applying the magnetic field and a ferromagnetic state spreads over a wider temperature region and the spin-glass state appears in only low temperatures with increasing magnetic field [4–6]. In contrast, the sign of θ_p of Y–Mn amorphous alloys is negative, indicating that the average exchange interaction is antiferromagnetic [10].

In both alloys mentioned above, the exchange interaction and the thermal variation of the amplitude of local magnetic moment arise from the itinerant characteristics of 3d electrons [8]. Y–Fe amorphous alloys exhibit an anomalous thermal expansion due to a large positive spontaneous volume magnetostriction [11, 12], whereas Y–Mn amorphous alloys scarcely show such a thermal expansion anomaly [8]. As is well known, the spontaneous volume magnetostriction is caused by a large thermal variation of the amplitude of the local magnetic moment [13, 14]. In Y–Fe amorphous alloy, therefore, the spin fluctuations are characterized by a significant thermal variation of amplitude of the local moment [8]. In contrast, the thermal variation of amplitude of the local moment is very small in Y–Mn amorphous alloys [8].

0953-8984/99/204053+10$19.50

Recently, it has been pointed out that the itinerant-electron magnetic properties of amorphous 3d transition metal based alloys can be discussed by taking the 3d-electron number N into consideration [15]. In itinerant-electron magnetic amorphous alloy systems, spin fluctuations whose characteristics change with N play an important role in magnetic properties. Therefore, the above mentioned spin-glass behaviour and spin fluctuation characteristics of both Y–Fe and Y–Mn amorphous alloys should be discussed comprehensively. Accordingly, $Y_{20}(Mn_{1-x}Fe_x)_{80}$ quasi-binary amorphous alloys are useful for the systematic study of magnetic properties by changing the 3d-electron number N.

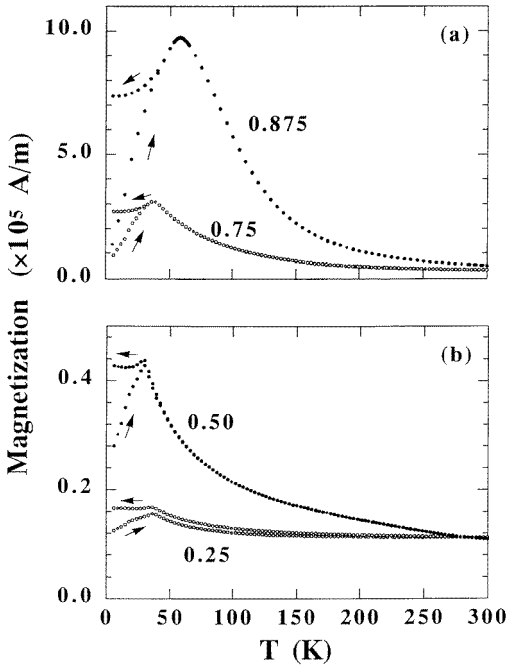

Figure 1. Field and zero-field cooling curves between 4.2 K and 300 K for $Y_{20}(Mn_{1-x}Fe_x)_{80}$ amorphous alloys. (a) $x = 0.875$ and 0.75, (b) $x = 0.50$ and 0.25.

In the present study, the spin-glass behaviour and the spontaneous volume magnetostriction of $Y_{20}(Mn_{1-x}Fe_x)_{80}$ amorphous alloys are investigated. The concentration dependence of the spin freezing temperature, the paramagnetic Curie temperature and the effective magnetic moment is discussed. Furthermore the thermal expansion anomaly above the Curie temperature is discussed in terms of the non-collective spin fluctuations, i.e. single-site spin fluctuations.

2. Experiment

The alloy targets were made by arc-melting in an Ar gas atmosphere. The amorphous alloys were prepared by high-rate DC sputtering on a water-cooled Cu substrate. The sputtering was continuously carried out for 2 days and the prepared sample thickness was about 0.3 mm. The Cu substrate was mechanically removed by grinding. Annealing was made at 523 K for 30 min in order to remove strains in the specimen.

Magnetic susceptibility measurements were made with a SQUID magnetometer (Quantum Design) in 0.01 T. AC magnetic susceptibility measurements were carried out by a mutual

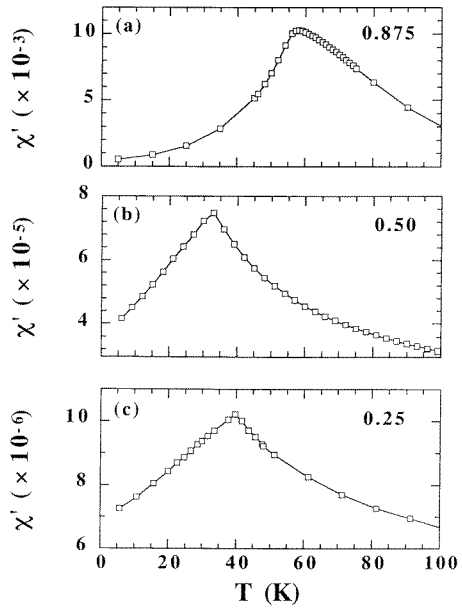

Figure 2. Temperature dependence of the AC magnetic susceptibility from 4.2 K to 100 K for $Y_{20}(Mn_{1-x}Fe_x)_{80}$ amorphous alloys with $x = 0.875$, 0.50 and 0.25 in (a), (b) and (c), respectively. Note that the scales of the ordinates are different from one another in magnitude.

inductance method in 0.001 T at 1000 Hz. The thermal expansion was measured with a differential transformer-type dilatometer.

3. Results and discussion

Magnetic cooling hysteresis curves of $Y_{20}(Mn_{1-x}Fe_x)_{80}$ amorphous alloys are shown in figures 1(a) and (b). These data were obtained in zero magnetic field (ZFC) and by cooling from the paramagnetic temperature region to liquid He temperature in the magnetic field of $H = 0.01$ T (FC). A significant hysteresis between FC and ZFC curves is observed at low temperatures. Figure 2 shows the real part of AC magnetic susceptibility χ' for $Y_{20}(Mn_{1-x}Fe_x)_{80}$ amorphous alloys with $x = 0.875$ in (a), 0.50 in (b) and 0.25 in (c). The existence of the spin-glass state in low temperatures was confirmed from hysteresis between ZFC and FC in figure 1 and a cusp of χ' in figure 2. The spin freezing temperature T_g is defined as the peak of χ', and the Curie temperature of $x = 1.00$ is determined from the higher inflection point of the thermomagnetization curve measured in 0.01 T. The resultant magnetic phase diagram is given in figure 3. A different magnetic phase diagram for rapidly quenched $Y_{20}(Mn_{1-x}Fe_x)_{80}$ amorphous alloys from the present result has been reported [16]. It has been pointed out that the magnetic properties of Y–Fe amorphous alloys greatly change by annealing [5], so that their magnetic properties are very sensitive to the structural relaxation. Since the cooling rate depends on the preparation method, the difference in the degree of the structural disorder would affect the magnetic properties. Moreover, the thermomagnetization of those rapidly quenched samples was measured in $H = 1.5$ T [16]. Such a high field suppress the spin freezing temperature T_g [4, 6].

The inset in figure 3 shows the magnetic phase diagram obtained by a finite-temperature theory of itinerant-electron magnetism of an amorphous system [15]. With increasing 3d-

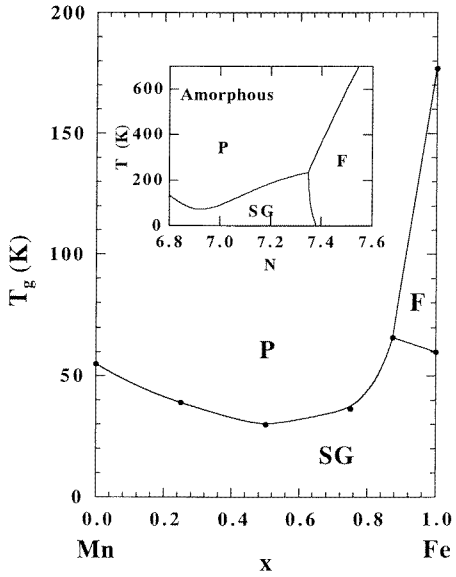

Figure 3. Concentration dependence of the spin freezing temperature T_g and the Curie temperature T_C for $Y_{20}(Mn_{1-x}Fe_x)_{80}$ amorphous alloys. The inset is the magnetic phase diagram calculated by a finite-temperature theory [15]. P: paramagnetic state, F: ferromagnetic state, SG: spin-glass state.

electron number N from $N = 6.8$, T_g shows a minimum and a re-entrant spin-glass state appears in the range of $N > 7.35$ [15]. It should be emphasized that the theoretical diagram is similar to the experimental phase diagram, even though the calculated transition temperatures are much higher than the experimental temperatures due to a molecular-field approximation. According to the theory, the onset condition for antiferromagnetism and ferromagnetism depends on the 3d-electron number N [15]. The average exchange interaction between the nearest-neighbour magnetic moment depends on the change of N. In the present study, the substitution of Fe for Mn means the increase in N; therefore, it is considered that the minimum of T_g is closely related to the change of the average exchange interaction. In order to see the sign of the average exchange interaction, we obtained the paramagnetic Curie temperature θ_p from the temperature dependence of the inverse magnetic susceptibility. The concentration dependence of θ_p and the effective magnetic moment P_{eff} is shown in figure 4. The sign of θ_p is negative in the Mn-rich concentration regions and becomes positive at around $x = 0.50$. These results imply that the ratio of the antiferromagnetic and ferromagnetic interactions is almost equal at around $x = 0.50$. The minimum of T_g occurs at the same concentration, suggesting that both antiferromagnetism and ferromagnetism are unstable.

The value of P_{eff} shows a steep concentration dependence in the range of $x > 0.50$, and becomes significantly large in the Fe-rich concentration region. It should be emphasized that the Curie–Weiss law in the itinerant-electron systems is different from that in the localized-magnetic-moment systems. The former is caused by the increase in the mean-square local amplitude of spin-density, i.e. spin fluctuations, with increasing temperature, accompanied by a large P_{eff} [13, 14]. On the other hand, the latter is caused by directional fluctuations of magnetic moments. According to the Curie-Weiss law, the magnetic moment P_c can be obtained from P_{eff} with the relation of

$$P_{eff}^2 = P_c(P_c + 2). \tag{1}$$

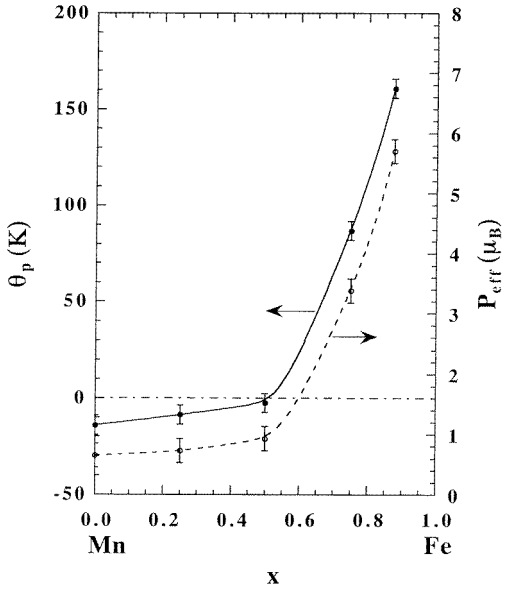

Figure 4. Concentration dependence of the paramagnetic Curie temperature θ_p and the effective magnetic moment P_{eff} for $Y_{20}(Mn_{1-x}Fe_x)_{80}$ amorphous alloys.

In the localized-magnetic-moment systems, the ratio of P_c to the saturation magnetic moment P_s is unity, i.e. $P_c/P_s = 1$. From the magnetization measurements up to 5.5 T at 4.2 K, P_s per 3d element evaluated from the law of approach to saturation is 0.9 μ_B and 0.5 μ_B for $x = 0.875$ and 0.75, respectively, and the P_c/P_s ratio is much larger than unity in the range of $x > 0.50$. Therefore, the thermal variation of spin fluctuations is significant in $x > 0.50$. Although P_s in the Mn-rich concentration region could not be obtained due to antiferromagnetic couplings, it is concluded that the small longitudinal thermal variation of spin fluctuations causes a small P_{eff}, compared with P_{eff}, in the Fe-rich concentration region.

The longitudinal thermal variation of mean-square amplitude of the local magnetic moment $\langle m^2 \rangle$ is accompanied by the spontaneous volume magnetostriction, where $\langle\ \rangle$ stands for the thermal average [17, 18]. Figure 5 shows the thermal expansion curves of the $Y_{20}(Mn_{1-x}Fe_x)_{80}$ amorphous alloys. The measured thermal expansion curves are given by the solid lines and the hypothetic non-magnetic curves are given by the dashed lines in the same figure. The total volume thermal expansion ω_{tot} is expressed as

$$\omega_{tot} = \omega_{ph} + \omega_{el} + \omega_s \tag{2}$$

where ω_{ph}, ω_{el} and ω_s are the phonon, the electron and the spontaneous volume magnetostriction terms, respectively. The non-magnetic terms of $\omega_{ph} + \omega_{el}$ in equation (2) are given by

$$\omega_{ph} + \omega_{el} = \Gamma\kappa \int (C_v^{ph} + C_v^{el})\, \mathrm{d}T \tag{3}$$

where C_v^{ph} and C_v^{el} are the specific heats of the phonon and electron terms, respectively, Γ the Grüneisen constant and κ the compressibility [19]. The value of C_v^{ph} is obtained from the Debye model. The Debye temperature Θ of $Ce_{20}Fe_{80}$ amorphous alloy has been reported to be 200 K [20], and then the same value is adapted to the present $Y_{20}Fe_{80}$ amorphous alloy. On the other hand, a nice fit with $\Theta = 300$ K for $Y_{20}Mn_{80}$ amorphous alloy has been reported [8].

For $Y_{20}(Mn_{1-x}Fe_x)_{80}$ amorphous alloys, the value of Θ is assumed as 225, 250 and 275 K for $x = 0.25$, 0.50 and 0.75 by a proportional partition with respect to x. The electron term C_v^{el} is generally proportional to the temperature T and the linear thermal expansion coefficient of electron term $\alpha_{el} = (1/3\omega_{el})(\partial\omega_{el}/\partial T)$ is about the order of 10^{-9} [19]. Therefore, the influence of C_v^{el} is very small, and the fitting including the T-linear term is scarcely different from the fitting without the linear term.

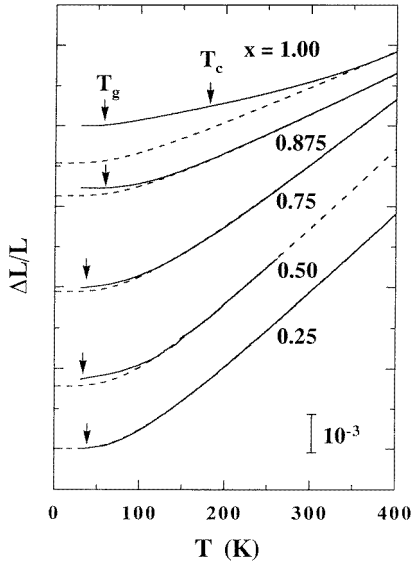

Figure 5. Thermal expansion curves of $Y_{20}(Mn_{1-x}Fe_x)_{80}$ amorphous alloys. The solid and dashed lines stand for the measured and hypothetical curves, respectively.

In high x regions, the solid line deviates from the dashed line at low temperatures, indicating a large ω_s. Figure 6 shows the temperature dependence of the spontaneous volume magnetostriction ω_s which is three times the difference between the solid and dashed lines in figure 5. The relation between ω_s and $\langle m^2 \rangle$ is given by [17, 18]

$$\omega_s(T) \propto \Gamma\kappa\langle m^2(T)\rangle. \tag{4}$$

It is clear that the spontaneous volume magnetostriction is significantly large and spreads over a wider temperature range in higher Fe concentrations. Therefore, the thermal variation of $\langle m^2 \rangle$ is very significant in Fe-rich concentration regions. The arrows in the figure indicate the transition temperatures obtained from figures 1 and 2. Note that there is no drastic change around the Curie temperature T_C as shown in the curves for $x = 1.00$, and even above T_C, a large ω_s is observed up to high temperatures. Similar behaviour is observed above the spin freezing temperature T_g as shown in figure 6. The decrease in $\langle m^2 \rangle$ in the paramagnetic temperature range can be expressed by the single-site spin fluctuation [21, 22]. The single-site spin fluctuation is non-collective spin fluctuation relating to the thermal excitation at the single-site. Therefore, the single-site spin fluctuation largely depends on the single-site magnetic energy structure. When the magnetic energy $E(m)$ shows an asymmetric structure with a sharp minimum and rapidly increases with increasing m in the paramagnetic temperature as seen from the inset in figure 6 which schematically shows the single-site magnetic energy structure in the paramagnetic temperature, the thermal excitation from the state with large m to that with small m occurs [21, 22], resulting in ω_s in the paramagnetic temperature range.

From figure 6, the effect of single-site spin fluctuation from large m to small m becomes more significant with increasing x.

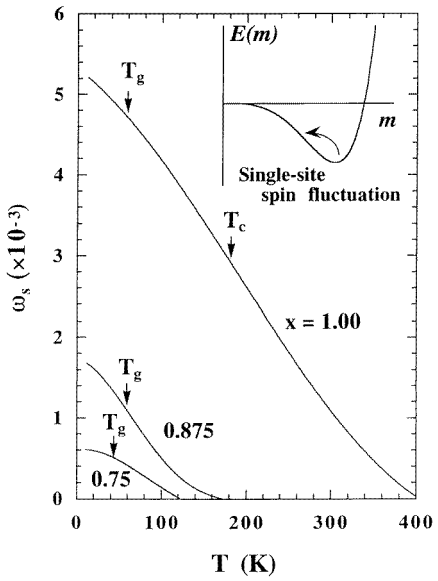

Figure 6. Temperature dependence of the spontaneous volume magnetostriction ω_s for $Y_{20}(Mn_{1-x}Fe_x)_{80}$ amorphous alloys. The inset shows a schematic single-site spin fluctuation in paramagnetic temperatures [21, 22].

The concentration dependence of the spontaneous volume magnetostriction $\omega_s(0)$ extrapolated to 0 K is shown in figure 7. With increasing x, $\omega_s(0)$ becomes larger, indicating the increase of the effect of the single-site spin fluctuation from large m to small m. On the other hand, there is no significant thermal variation of $\langle m^2 \rangle$ in Mn-rich concentration regions. The effect of the single-site spin fluctuation on the linear thermal expansion coefficient α has also been observed. In figure 8, the temperature dependence of α obtained from differential of the linear thermal expansion shown in figure 5 is shown by the solid lines and the hypothetical non-magnetic coefficient α_{hyp} by the dashed lines. Since the temperatures above 400 K are much higher than the Debye temperature, $\Theta = 200$–300 K, the phonon term C_v^{ph} should follow the Dulong–Petit law and converge to a constant value. As mentioned already, the contribution of C_v^{el} is very small. However, a large increment of α is conserved in high temperatures, showing the magnetic contribution caused by the thermal excitation to large m, especially in the Mn-rich concentration region. In the Fe-rich concentration regions, the single-site spin fluctuation from large m to small m exists at the paramagnetic temperature, therefore the linear coefficient of the spontaneous volume magnetostriction α_s becomes negative. These results imply the difference in the magnetic energy structure between the Mn- and Fe-rich concentration regions at the paramagnetic temperature. The value of α at 400 K gradually decreases with x, indicating that the value of α_s in the paramagnetic temperature region changes from positive to negative. Therefore, the effect of the single-site spin fluctuation from large m to small m becomes more significant in a higher range of x.

$Y_{20}(Mn_{1-x}Fe_x)_{80}$ amorphous alloys show the spin-glass behaviour at low temperatures. As is well known, in the spin-glass state, the value of exchange interaction has a wide distribution spread over from antiferromagnetic to ferromagnetic interaction. In the present

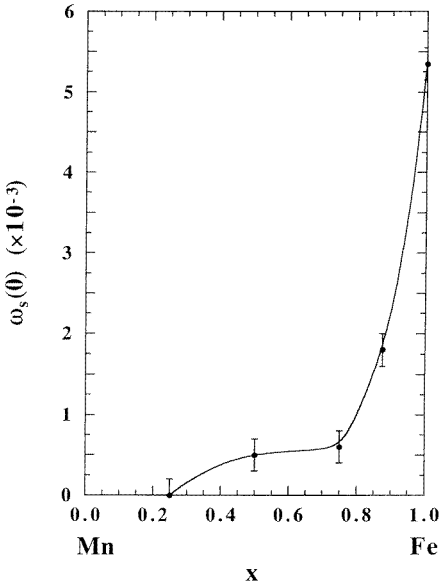

Figure 7. Concentration dependence of the spontaneous volume magnetostriction at 0 K, $\omega_s(0)$, for $Y_{20}(Mn_{1-x}Fe_x)_{80}$ amorphous alloys.

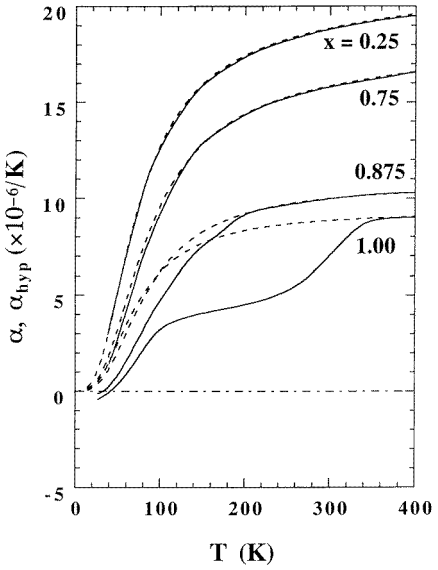

Figure 8. Temperature dependence of the linear thermal expansion coefficient for $Y_{20}(Mn_{1-x}Fe_x)_{80}$ amorphous alloys. The measured coefficient α and the hypothetic coefficient α_{hyp} are respectively given by the solid and dashed lines.

spin-glass amorphous alloy system, the distribution of the exchange interactions and the variety of the energy structure come from the variety of the local-site condition due to a structural disorder [15]. The local-site condition is characterized by the 3d-electron number N and the interatomic distance from the central atom to the surrounding atoms [15]. In the present

study, N varies with x, and we assumed that the degree of structural disorder scarcely changes with changing x, because the samples were prepared by sputtering under the same condition. The averaged density of states at the Fermi level is small and satisfies the onset condition of antiferromagnetic interaction when N is small, then most local sites show antiferromagnetic coupling irrespective of the interatomic distance for each local site [15]. With increasing N, the structural averaged density of states at the Fermi level increases and approaches the Stoner condition [15]. Even if the structural averaged density of states at the Fermi level does not satisfy the Stoner condition, the ferromagnetic coupling appears at the local site with the wider interatomic distance than the average interatomic distance [15], since the transfer energy of 3d electrons is larger at the wider interatomic distance site. At such a local site, the magnetic energy curve shows an asymmetric structure with a sharp minimum and rapidly increases with the magnitude of m as shown in the inset of figure 6 [15]. The effect of the single-site spin fluctuation from large m to small m increases when the asymmetric sharp energy minimum becomes more significant with increasing N, resulting in a large thermal variation of $\langle m^2 \rangle$. Taking theoretical results into account, the present experimental results can be explained by the gradual change of the sign of average exchange interaction given in figure 4 and the magnetic energy structure change as a result of the change of the density of states at the Fermi level of each local site with changing N.

4. Conclusion

We have investigated the variations of the magnetic properties of $Y_{20}(Mn_{1-x}Fe_x)_{80}$ amorphous alloys by changing the 3d-electron number. The systematic variation of the paramagnetic Curie temperature, the effective magnetic moment and the spontaneous volume magnetostriction have been observed. These results have been discussed in terms of single-site spin fluctuations. The main results are summarized as follows.

(a) The spin freezing temperature T_g shows a minimum at around $x = 0.50$. This behaviour is explained by the change in the sign of the average exchange interaction from negative to positive with increasing x. The magnetic phase diagram is qualitatively consistent with the theoretical one.

(b) The concentration dependence of the paramagnetic Curie temperature θ_p and the effective magnetic moment P_{eff} shows a marked change at around $x = 0.50$.

(c) The spontaneous volume magnetostriction at 0 K indicates a significant concentration dependence and fades away around $x = 0.25$.

(d) In the Fe-rich concentration region, a large thermal variation of $\langle m^2 \rangle$ due to spin fluctuations is observed in low temperatures. In addition, $Y_{20}Fe_{80}$ amorphous alloy exhibits a large spontaneous volume magnetostriction even above the Curie temperature T_C due to the single-site spin fluctuation in the paramagnetic temperature region.

(e) The linear thermal expansion coefficient α at 400 K decreases with increasing x, indicating the different spin fluctuation characteristics between the Mn-rich and the Fe-rich regions.

Acknowledgment

One of the authors (AF) would like to thank the Research Fellowships of the Japan Society for the Promotion of Science for Young Scientists for financial support.

References

[1] Forester D W, Koon N C, Schelleng J H and Rhyne J J 1979 *Solid State Commun.* **30** 177
[2] Forester D W, Koon N C, Schelleng J H and Rhyne J J 1979 *J. Appl. Phys.* **50** 7336
[3] Coey J M D, Givord D, Liénard A and Rebouillat J P 1981 *J. Phys. F: Met. Phys.* **11** 2707
[4] Fujita A, Komatsu H, Fukamichi K and Goto T 1994 *J. Phys.: Condens. Matter* **5** 3003
[5] Suzuki T, Fujita A, Fukamichi K and Goto T 1994 *J. Phys.: Condens. Matter* **6** 5741
[6] Fukamichi K, Fujita A and Suzuki T 1995 *Sci. Rep. RITU* A **41** 41
[7] Tange H, Ikeda M, Ono T, Kamimori T and Goto M 1995 *J. Magn. Magn. Mater.* **140–144** 285
[8] Fujita A, Suzuki T, Fukamichi K, Obi Y and Fujimori H 1995 *Mater. Trans. JIM* **36** 852
[9] Obi Y, Kamiguchi Y, Morita H and Fujimori H 1987 *J. Phys. Soc. Japan* **56** 1623
[10] Obi Y, Kondo S, Morita H and Fujimori H 1988 *J. Physique Coll.* **49** C81097
[11] Fujita A, Suzuki T, Kataoka N and Fukamichi K 1994 *Phys. Rev.* B **50** 6199
[12] Suzuki T, Fujita A, Chiang T H and Fukamichi K 1994 *Mater. Sci. Eng.* A **181/182** 954
[13] Moriya T and Usami K 1980 *Solid State Commun.* **34** 95
[14] Moriya T 1985 *Spin Fluctuations in Itinerant Electron Magnetism (Springer Series in Solid-State Sciences 56)* (Berlin: Springer)
[15] Kakehashi Y 1991 *Phys. Rev.* B **43** 10 820
[16] Ishio S and Fujikura M 1988 *Z. Phys. Chem., NF* **157** 301
[17] Kakehashi Y 1989 *Physica* B **161** 143
[18] Kakehashi Y 1980 *J. Phys. Soc. Japan* **49** 2421
[19] Touloukian Y S, Kirby R K, Taylor R E and Desai P D 1975 *Thermal Expansion—Metallic Elements and Alloys (TPRC Data Series, Thermal Properties of Matter 12)* (New York: IFI–Plenum) p 1
[20] Chiang T H, Komatsu H, Matsunaga A and Fukamichi K 1994 *Mater. Sci. Eng.* A **181/182** 958
[21] Hasegawa H 1980 *J. Phys. Soc. Japan* **49** 178
[22] Kakehashi Y 1981 *J. Phys. Soc. Japan* **50** 1925